Available online at www.sciencedirect.com
SCIENCE DIRECT
Journal of Molecular Structure 742 (2005) 21–29
Journal of MOLECULAR STRUCTURE
www.elsevier.com/locate/molstruc

Rotational analysis of several bands in the high-resolution infrared spectrum of butadiene-1-$^{13}C_1$: assignment of vibrational fundamentals

Norman C. Craig[a,*], Keith A. Hanson[a], Michael C. Moore[a], Robert L. Sams[b]

[a]*Department of Chemistry, Oberlin College, Science Center A263, 119 Woodland St., Oberlin, OH 44074-1097, USA*
[b]*Environmental and Molecular Sciences Laboratory, Pacific Northwest National Laboratory, P.O. Box 999, Mail Stop K8-88, Richland, WA 99352, USA*

Received 10 September 2004; revised 13 November 2004; accepted 15 November 2004
Available online 10 February 2005

Abstract

Butadiene-1-$^{13}C_1$ was synthesized, and its high-resolution (0.002 cm^{-1}) infrared spectrum was recorded for several bands in the mid-infrared region. A complete analysis of the rotational structure in the C-type band at 524.485 cm^{-1} for CH_2 twisting and a partial analysis of the rotational structure in the C-type bands at 900.0 and 909 cm^{-1} were performed. Of these latter two bands, which are of comparable intensity, the higher frequency one is largely CH_2 out-of-plane wagging and the lower frequency one is largely $^{13}CH_2$ out-of-plane wagging. Taken together these bands correlate with one infrared-active a_u fundamental and one Raman-active b_g fundamental of butadiene. The ground state rotational constants are $A = 1.3887919$ (6), $B = 0.1436683$ (3), and $C = 0.1302251$ (3) cm^{-1}, and upper state rotational constants are reported for the bands at 524.485 and 900.0 cm^{-1}. Medium resolution infrared and Raman spectra gave a complete assignment of the vibrational fundamentals, including 11 fundamentals observed directly for the first time.

Keywords: High-resolution infrared spectroscopy; Raman spectra; Rotational constants; Quantum chemical calculations; Structural parameters

1. Introduction

The overall goal of this research is to obtain an equilibrium structure of butadiene (BDE) by the combined spectroscopic-quantum chemical (QC) method. Because BDE is a nonpolar molecule, the analysis of rotational structure in high-resolution infrared (IR) spectra is required. The subject of this paper, butadiene-1-$^{13}C_1$ (BDE-1-$^{13}C_1$), is one of two carbon-13 species needed for the structural study. Another carbon-13 species, BDE-2,3-$^{13}C_2$, has been synthesized, and the investigation of its high-resolution IR spectrum has been launched.

Obtaining equilibrium structures by the combined spectroscopic-QC method for molecules as large as butadiene is now feasible [1–5]. Not only does this method depend on finding ground state rotational constants for a full set of isotopomers, but it also benefits from the careful determination of the force field at the quadratic and cubic levels by the interplay of experiment and theory. These force constants are used in the QC computation of vibration–rotation constants. Thus, an important component of this project has been improving and extending knowledge of the vibrational fundamentals of the isotopomers of butadiene. The current paper provides a complete assignment of the vibrational fundamentals of BDE-1-$^{13}C_1$ for the first time. These assignments are reinforced by calculations of the frequencies and intensities with a B3LYP/6-311++G(d,p) model. Ground state rotational constants and improved vibrational fundamentals are now available from IR investigations of BDE itself [6], BDE-2,3-d_2 [6], BDE-*trans*,*trans*-1,4-d_2 [7], BDE-*cis*,*cis*-1,4-d_2 [7], and BDE-*cis*,*trans*-1,4-d_2 [7]. Ground state rotational constants for BDE-1,1-d_2 were obtained from a microwave investigation of this slightly polar species [8]. Very recently, Halonen et al. [9] have obtained rigid-rotor rotational constants for butadiene from a very high-resolution investigation in the CH-stretching region. They used tunable laser spectroscopy and a cold jet-beam. Sun et al. have used sub-Doppler Lamb-dip spectroscopy to investigate lines in several ^RQ_K branches

* Corresponding author. Tel.: +1 440 775 8664; fax: +1 440 775 6682.
E-mail address: norm.craig@oberlin.edu (N.C. Craig).

0022-2860/$ - see front matter © 2005 Elsevier B.V. All rights reserved.
doi:10.1016/j.molstruc.2004.11.090

in the IR spectrum of butadiene and have combined this high accuracy data with the published data [6] to obtain an improved rotational Hamiltonian for the ground state and ν_{11} [10].

Interest in the equilibrium structure arises from asking if the structure of the carbon backbone of butadiene reflects partial delocalization of the pi electrons. Thus, is the CC 'double' bond longer than the localized double bond in ethylene, and is the CC 'single' bond shorter than an sp^2–sp^2 single bond? As described in a previous paper, the results of an electron diffraction study are ambiguous [7,11], and supplementing the electron diffraction results with a microwave investigation of BDE-1,1-d_2 leaves the answer in doubt [8]. QC structures computed with an MP2/6-311++G(d,p) model and a B3LYP/6-311++G(d,p) model have differences that cloud the answer as well [7]. An equilibrium structure, rather than a ground state structure of the r_0 type or a substitution structure of the r_s type, is needed to remove the confusing contributions of ground-state vibrational motion from the structure. Also, an equilibrium structure may be used to evaluate structures predicted by purely QC calculations.

BDE-1-$^{13}C_1$ has reduced C_s symmetry in comparison with the higher C_{2h} symmetry of butadiene and most of the isotopomers that have been investigated. As a consequence, some modes, which are only Raman active for BDE, light up in the IR spectrum of BDE-1-$^{13}C_1$. We have investigated the rotational structure in one dramatic example of this type in the spectrum of BDE-1-$^{13}C_1$. Less favorably, the relaxed selection rules for BDE-1-$^{13}C_1$ allow more instances of resonances.

Some vibrational spectroscopy, including an analysis of fundamentals, has been done on BDE-1-$^{13}C_1$ before [12,13]. We have synthesized this substance by following a method previously used for making carbon-13-labeled isoprene [14]. This method uses the Wittig reaction to replace the carbonyl function in acrolein with a $=^{13}CH_2$ grouping by reaction with the ylide made from (methyl-$^{13}C_1$)-triphenylphosphonium iodide and sodium hydride.

2. Experimental section

Preparations for the synthesis of BDE-1-$^{13}C_1$ were carried in a plastic glove bag purged with dry nitrogen. In a typical reaction 0.35 g (8.8 mmol) of sodium hydride (60% dispersion in mineral oil, Aldrich) was dissolved in 10 mL of anhydrous dimethylsulfoxide (DMSO, Aldrich) in a three-neck (14/20 joints), 50-mL flask containing a stir bar. Three grams (7.4 mmol) of (methyl-^{13}C)triphenylphosphonium iodide (99 at.%, Aldrich) was dissolved in 15 mL of DMSO in a 25-mL, pressure-equalizing addition funnel equipped with a greased stopcock. The funnel was attached to the flask through one joint. A serum bottle cap was placed in another joint. Through the middle joint a tube equipped with a stopcock led to a trap joined by ball joints and equipped with two stopcocks. The system was filled with dry nitrogen. The trap was cooled in pentane slush (−125 °C) to freeze out any butadiene emitted. The solution was heated to 70 °C for about an hour until hydrogen gas evolution from reaction of sodium hydride with residual water ceased. After cooling to room temperature, the solution of the phosphonium salt was added dropwise to give a colored solution of the ylide. With a gas-tight syringe 0.55 mL (<8.2 mmol) of acrolein (90%, Aldrich), which had been dried by distillation through a P_2O_5-and-glass-wool-packed column, was injected into the reaction mixture, which was stirred for 1 h. Following a gentle purge with dry nitrogen gas, the stopcocks were closed. The cold trap was attached to a vacuum system and cooled in liquid nitrogen, while pumping nitrogen gas away from any frozen-out butadiene. Most of the product butadiene was obtained when the reaction vessel and the addition funnel were fitted with greased plugs and the connecting tube was attached to the vacuum system and the volatiles were removed, as the reaction mixture was vigorously stirred.

The yield of butadiene-1-$^{13}C_1$ was a disappointing 5–10% after GC purification at room temperature on a 5-m column containing tricresylphosphate on Fluoropak (fine Teflon particles). Despite a number of attempts at this reaction with unlabeled and labeled material and with rigorously dry conditions, we were unable to improve the yield on the small scale. The analysis of the rotational structure in the high-resolution IR spectrum confirmed that the substance synthesized was the 1-$^{13}C_1$ species. The medium-resolution IR spectrum showed that the isotopic purity was not compromised in the synthesis.

2.1. High-resolution spectroscopy

High-resolution IR spectra were recorded with a resolution of 0.0020 cm^{-1} (0.9/MOPD) on a Bruker IFS 120HR spectrometer at PNNL. Details of the use of this instrument at PNNL have been described recently [15]. Interferograms were transformed without apodization.

Samples were examined at room temperature in a White cell set to a path length of 16 m. Spectra used in the rotational analysis were obtained with 512 scans as follows: (1) 1176–780 cm^{-1}, 0.116 Torr, zero filling (z.f.) of 4; (2) 604–451 cm^{-1}, 0.5 Torr, z.f. of 4. For the higher-frequency spectrum the detector was a liquid-nitrogen–cooled mercury–cadmium–telluride device; for the lower-frequency spectrum the detector was a liquid-helium–cooled silicon bolometer.

Calibration of the spectrometer was done with CO_2 or H_2O lines [15].

2.2. Medium-resolution spectroscopy

Mid-IR spectra of gases were recorded on a Nicolet 760 Magna spectrometer at 0.1-cm^{-1} resolution in a 10-cm cell equipped with potassium bromide windows. Far-IR

gas-phase spectra were recorded on a Perkin–Elmer 1700X spectrometer at 1-cm^{-1} resolution in a 10-cm cell equipped with polyethylene windows. The far-IR spectrometer was purged with dry nitrogen. Boxcar apodization was used for both instruments.

Raman spectra were recorded with a Raman accessory module attached to the Nicolet 760 spectrometer. Excitation was with the 1064-nm line of a Nd:YVO_4 laser at a power of about 0.5 W at the sample, and detection was with a liquid-nitrogen–cooled germanium device. Samples were sealed in standard-wall, 1.8-mm Kimax capillaries and examined as pressurized liquids at room temperature. The 90° optical system was used with a polarization analyzer in the collection optics. Resolution was 4 cm^{-1}, and 2000 scans were accumulated for 0 and 90° settings of the polarization analyzer. Another spectrum with 1000 scans at 2-cm^{-1} resolution was recorded with the more efficient 180° optical system to confirm weak bands and give better resolution of overlapped features. Raman frequencies have an uncertainty of ± 1 cm^{-1}.

3. Symmetry and complete assignment of fundamentals

BDE-1-$^{13}C_1$ has lower, C_s, symmetry than most of the other butadienes which have been fully investigated. They have C_{2h} symmetry. As a consequence, all vibrational fundamentals of BDE-1-$^{13}C_1$ have IR-active bands as well as Raman-active bands. The principal axes of rotation line up approximately as shown in Fig. 1. (Though schematic, Fig. 1 shows the location of the principal axes more faithfully than in our previous papers [6,7].) The molecule is a near prolate top with $\kappa = -0.9786$. The out-of-plane vibrations of the a'' symmetry species have dipole moment changes along the c-axis and thus IR bands of C-type shape in the gas phase. The in-plane modes of the a' symmetry species have, in general, dipole moment components along both the a- and b-axes and thus have IR bands of hybrid A/B-shape in the gas phase. The Raman bands of the a' symmetry species are polarized, and the Raman bands of the a'' symmetry species are depolarized.

The only previous investigation of a vibrational spectrum of BDE-1-$^{13}C_1$ was a mid-IR study of matrix-isolated material by Huber-Wälchli and Günthard [12]. Our investigation of the gas-phase IR spectrum and the liquid-phase Raman spectrum extended the earlier work and provided a complete assignment of the vibrational fundamentals. The mid-IR spectrum of BDE-1-$^{13}C_1$ in the gas phase is available in Supplementary Fig. 1aS and bS, and the far-IR spectrum is in Supplementary Fig. 2S. The Raman spectrum of the liquid phase of BDE-1-$^{13}C_1$, as recorded with 90° optics, is in Supplementary Fig. 3S. Traces are shown for both settings of the polarizer in the scattered light beam.

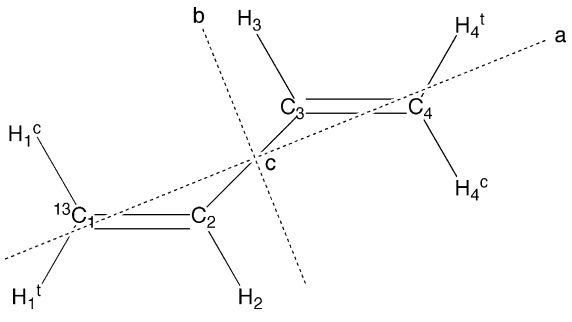

Fig. 1. Schematic of the structure of butadiene-1-$^{13}C_1$.

Table 1 gives the new assignments of vibrational fundamentals of BDE-1-$^{13}C_1$ in comparison with the assignments for the normal species and the previous fragmentary assignment from the IR spectrum of the argon-matrix study [12]. This table includes the frequencies computed by Panchenko et al. [13] for both species using an MP2/6-31G* model to predict force constants, which were subsequently scaled to fit the observed frequencies for the normal species. The numbering and approximate descriptions of the fundamentals are from Panchenko et al. with a minor exception for ν_2 and ν_3. Most of the observed frequencies for the normal species are drawn from the literature [13] as slightly revised in our earlier study [6]. Based on new spectral observations for the 2,3-$^{13}C_2$ isotopomer of butadiene, for which Fermi resonance also plays a significant role in the CH-stretching region, we have revised several assignments in the CH-stretching region of the normal species. We also note that the recent high-resolution investigation of Halonen et al. [9] confirmed the assignment of ν_{17} near 3100.6 cm^{-1}. For the new observations for BDE-1-$^{13}C_1$ in Table 1, information is supplied about relative intensities, shapes of bands in the gas-phase IR spectrum, and polarizations in the liquid-phase Raman spectrum. Frequencies for eleven directly observed fundamentals are reported for the first time. Four of the frequencies derived by Huber-Wälchli and Günthard [12] from combination tones are supported by the new direct observations. Three of the frequencies for BDE-1-$^{13}C_1$ in Table 1 are adjusted for Fermi resonance. The overall agreement between the calculated and observed fundamental frequencies for BDE-1-$^{13}C_1$ is quite good.

The last two columns in Table 1 give the observed and calculated isotopic shifts [13] between the frequencies for the normal and ^{13}C species. For use in computing isotopic shifts with the new experimental data, the frequencies supplied for the a_g modes of the normal species are for liquid-phase Raman spectra [6]. The predictions for these shifts are expected to be reliable. Thus, a comparison of the predicted and observed shifts is a strong test of the consistency of the assignments for the two isotopomers. With the exception of ν_2, agreement between the predicted and observed shifts lies within experimental uncertainties. Larger uncertainties in frequencies of the very weak bands for the 'b_g' modes of both species in the liquid-phase Raman

Table 1
Observed and calculated vibrational fundamentals for butadiene and butadiene-1-$^{13}C_1$ (cm^{-1})

	Approx. normal coord.[a]	d_0		$1\text{-}^{13}C_1$			Δ	
		Obsd.[b]	Calc.[a]	Lit.[c]	Obsd.[d]	Calc.[a]	Obsd.	Calc.[a]
a_g	ν_1 $\nu(CH_2)$ a str	3092	3111	3091	3080[e] w, pol	3098	−12	−13
	ν_2 $\nu(CH_2)$ s str[f]	3002	3024		3001 s, pol	3019	−1	−5
	ν_3 ν(C–H) s str[f]	3002	3008		3001 s, pol	3008		0
	ν_4 ν(C=C) s str	1639	1652	1638	1633 vs, pol	1645	−6	−7
	ν_5 $\delta(CH_2)$ sci	1439	1443		1437 m, pol	1441	−2	−2
	ν_6 δ(C–H) def	1285[g]	1287	1282	1280[g] m, pol	1280	−5	−7
	ν_7 ν(C–C) str	1203	1209	(1210)	1202 m, pol	1208	−1	−1
	ν_8 $\rho(CH_2)$ rock	890	879		887 w, pol	876	−3	−3
	ν_9 δ(C=C–C) def	514	510	(504)	511 m, pol	506	−3	− 4
a_u	ν_{10} χ(C–H) wag	1014	1022	1024	1014 s, C	1021	0	−1
	ν_{11} $\chi(CH_2)$ wag	908	907	898	900 s, C	899	−8	−8
	ν_{12} $\tau(CH_2)$ twist	524.5	518	536	524.5 m, C	518	0	0
	ν_{13} τ(C–C) tors	162.5	159		162 w, C	158	−0.5	−1
b_g	ν_{14} χ(C–H) wag	967	964	(967)	968 vw	964	+1	0
	ν_{15} $\chi(CH_2)$ wag	909	908	906	909 s, C	908	0	0
	ν_{16} $\tau(CH_2)$ twist	750	747		752 vw	747	+2	0
b_u	ν_{17} νCH$_2$) a str	3100.6[h]	3111		3099[i] s, B	3111	−1.6	0
	ν_{18} ν(C–H) str	3023[g]	3024	3026	3022[g] m, B	3024	−2	0
	ν_{19} $\nu(CH_2)$ s str	3013	3015		~3005[j] m, B	3014	−2	−1
	ν_{20} ν(C=C) a str	1596	1591	1582	1582 s, A	1577	−14	−14
	ν_{21} $\delta(CH_2)$ sci	1381	1380	1380	1380 m, A	1380	−1	0
	ν_{22} δ(C–H) def	1281[f]	1290	1305	1280[f] w, B	1289	−1	−1
	ν_{23} $\rho(CH_2)$ rock	990	996	985	988 m, B?	993	−2	−3
	ν_{24} δC=C–C) def	299	295	301	298 wm, B	293	−1	−2

[a] Ref. [13].
[b] Ref. [6]. Liquid-phase Raman spectrum for a_g and b_g modes; gas-phase IR spectrum for a_u and b_u modes. The decomposition of Fermi resonance for ν_{18} has been revised.
[c] Ref. [12]. Values in parentheses were derived from combination tones.
[d] Raman liquid phase for all 'a_g' modes and for ν_{14} and ν_{16} 'b_g' modes. Intensities (w, weak; m, medium; s, strong); pol, polarized; band shapes. In gas-phase IR, $\nu_1 = 3085$, $\nu_4 = 1640$, and $\nu_{17} = 3102\ cm^{-1}$.
[e] 3085 cm^{-1} in gas-phase IR spectrum. $^{13}CH_2$ stretch.
[f] Designations for ν_2 and ν_3 have been exchanged.
[g] Adjusted for Fermi resonance. For BDE-1-$^{13}C_1$: 1298, 1275, first 0.42 intensity of second; 3046, 2982, first 1.64 the absorbance of the second; 1291, 1270, equal intensities.
[h] Ref. [9].
[i] 3092 cm^{-1} in liquid-phase Raman spectrum. $^{12}CH_2$ stretch.
[j] 2994 cm^{-1} in liquid-phase Raman spectrum.

spectrum explain the unexpected positive isotope shifts. Because of Fermi resonances in the CH-stretching region, the assignments in this region of the spectrum remain tentative.

A striking difference between the IR spectra of the BDE-1-$^{13}C_1$ species and the normal species is how ν_{15} lights up in the IR spectrum of BDE-1-$^{13}C_1$. A comparable mode for the normal species belongs to the b_g symmetry species and is only Raman active. This mode for the normal species is almost degenerate with ν_{11} of the IR-active a_u symmetry species. The frequency difference between these modes in the IR spectrum of the ^{13}C species becomes 9 cm^{-1}. Two bands with nearly equal intensities appear as well in the Raman spectrum. A normal coordinate analysis by Panchenko [16] and subsequently by us with the B3LYP/6-311++G(d,p) model [17] shows that the lower frequency mode is largely flapping of the $^{13}CH_2$ end of the molecule, whereas the higher frequency mode is largely flapping of the $^{12}CH_2$ end of the molecule. The other two modes of the ^{13}C species that correlate with b_g modes of the normal species remain unobservable in the IR spectrum. A second example of the significant effect of the lowered symmetry BDE-1-$^{13}C_1$ occurs for the two highest frequency CH stretching modes. In the gas-phase IR spectrum a band for the $^{12}CH_2$ stretching mode is at 3099 cm^{-1}, whereas the band for the $^{13}CH_2$ stretching mode is at 3085 cm^{-1}. The corresponding liquid-phase Raman frequencies are 3092 and 3080 cm^{-1}. The near coincidence of ν_6 and ν_{22} in the CH-bending region is, however, accidental.

Supplementary Table 1S contains all the assignments for the vibrational transitions of BDE-1-$^{13}C_1$ obtained from the IR and Raman spectra. This table includes the unscaled predictions of frequencies and infrared and Raman intensities computed with the B3LYP/6-311++G(d,p) model [17].

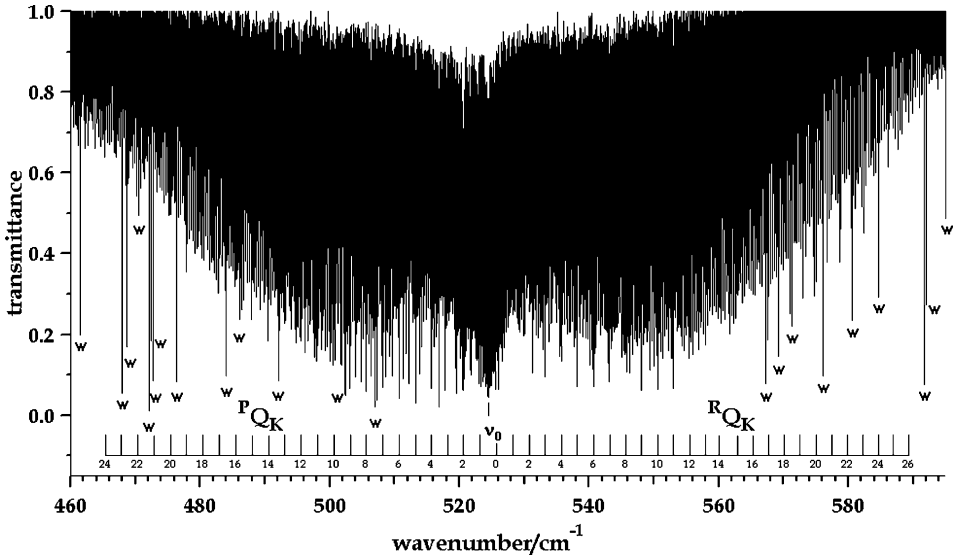

Fig. 2. Overall structure of the C-type band of butadiene-1-$^{13}C_1$ at 524.5 cm^{-1} due to the ν_{12} mode for CH_2 twisting. The 'w' symbol designates extraneous lines from water vapor.

4. Analysis of high-resolution spectra

The rotational structure was analyzed in three bands of BDE-1-$^{13}C_1$, which is nearly a prolate symmetric top with $\kappa = -0.9786$. The structure in the C-type band at 524.485 cm^{-1}, which arises from CH_2 twisting, was the most thoroughly analyzed. For the pair of overlapping C-type bands at 900.0 and 909 cm^{-1} the more intense, lower frequency band was analyzed for subbands with $K'_a = 3$ outward. A limited investigation of the band at 909 cm^{-1} was done. The lower frequency band is for $^{13}CH_2$ flapping; the higher frequency band is for $^{12}CH_2$ flapping.

Selection rules for C-type bands and the strategy for making assignments were reviewed recently [6]. We made extensive use of the Loomis–Wood pattern recognition program to identify subband series and to manage the large data sets [18]. A number of supporting FORTRAN programs were used in making the assignments as were Arthur Maki's ASYMBD programs for fitting spectral lines and predicting spectra. Christopher Neese's add-ins for Excel and Igor were useful in displaying predictions of subband series in an organized manner and in presenting spectral data in graphical formats [19].

For fitting rotational states a Watson-type Hamiltonian was used with the asymmetric rotor reduction and an I^r representation. All the quartic centrifugal distortion constants were fit unless otherwise noted. Ground state (GS) rotational constants were fit to ground state

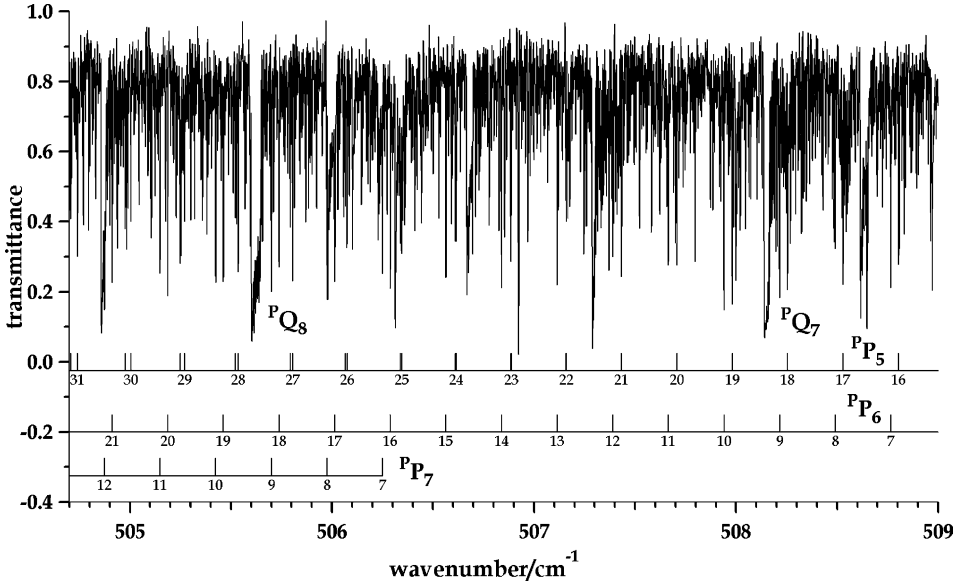

Fig. 3. An example of details of the assignment in the P branch of the band for ν_{12} in the vicinity of $^{P}Q_7$ and $^{P}Q_8$.

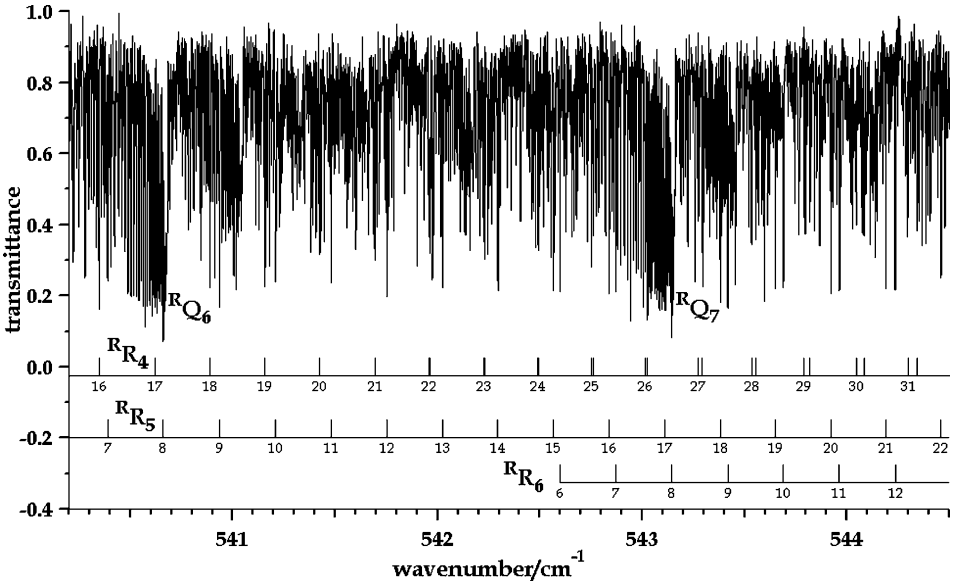

Fig. 4. An example of details of the assignment in the R branch of the band for ν_{12} in the vicinity of $^{R}Q_6$ and $^{R}Q_7$.

combination differences (GSCDs). The GS constants were held while fitting upper state (US) constants to lines.

The first band to be discussed is the C-type band at 524.485 cm^{-1} for $\nu_{12}(a'')$, which was thoroughly analyzed. Fig. 2 shows the overall appearance of this band and gives combs marking the $^{P}Q_K$ and $^{R}Q_K$ features from the band center to the wings of the band. Extraneous lines due to water are marked with a 'w'. Fig. 3 is an example of the details of the assignment of $^{P}P_K$ subbands in the vicinity of $^{P}Q_7$ and $^{P}Q_8$, where the onset of K_c-splitting of $^{P}P_5$ appears. Fig. 4 is a sample of the details of the assignment of $^{R}R_K$ subbands in the vicinity of the $^{R}Q_6$ and $^{R}Q_7$ features, where the onset of K_c-splitting of $^{R}R_4$ appears. Subband assignments included $^{R}R_0$ to $^{R}R_{26}$, $^{R}Q_0$ to $^{R}Q_4$, $^{P}P_1$ to $^{P}P_{24}$, and $^{P}Q_1$ to $^{P}Q_6$. In addition, the offside series $^{R}P_0$ and $^{P}R_1$ were assigned. A total of 2843 lines were assigned in this band from which 1305 GSCDs were derived. We used low-K_c ($K_c = J - K_a$) as the default assignment where high-K_c ($K_c = J + 1 - K_a$) lines were not resolved, and in computing GSCDs we avoided using lines redundantly. Table 2 gives the rotational constants fit to these GSCDs for ν_{12} and for the other two C-type bands. The total number of GSCDs was 2181. Of the GSCDs 60% came from the band for ν_{12}, 33% from the band for ν_{11}, and 7% from the band for ν_{15}. A perturbation prevented fitting US rotational constants from $K'_a = 6$, $J' = 25$ outward in J and K in the band for ν_{12}. For the interior part of this band US rotational constants were fit to 1219 lines. The results of this fit are given in Table 2.

The lines assigned for the C-type band of BDE-1-$^{13}C_1$ at 524.484 cm^{-1} are given in several Supplementary tables. Table 2S contains the GSCDs from ν_{12} and the details of their fitting to rotational constants. Table 3S contains the lines with $K'_a \leq 6$, $J' \leq 25$ and the details of their fitting to US constants. Table 4S contains the 1623 lines from $K_a = 6$ outward, which were assigned to the C-type band.

The overall structure of the two, overlapping C-type bands near 900 cm^{-1} is shown in Fig. 5. The band centered at 900.0 cm^{-1} is for ν_{11}, the $^{13}CH_2$ flapping mode. The band centered at 909 cm^{-1} is for ν_{15}, the $^{12}CH_2$ flapping mode. Though not obvious in Fig. 5, the lower frequency band has the higher intensity. As its combs for $^{P}Q_K$ and $^{R}Q_K$ features indicate, the lower frequency band was extensively analyzed. Subbands for $K'_a = 3$ outward were assigned. Congestion in the band center and a perturbation interfered with extending the analysis all the way to the band center. For the band centered at 909 cm^{-1} for ν_{15}, the combs for this band in Fig. 5 show the analysis was limited to subbands with $K'_a = 4$–8.

Focusing on the C-type band for ν_{11} at 900 cm^{-1}, we provide a sample of the details of the assignment in the R

Table 2
Rotational constants for butadiene-1-$^{13}C_1$

	Ground state[a,b]	$\nu_{12}=1$[a]	$\nu_{11}=1$[a]
A (cm^{-1})	1.3887919 (6)	1.387343 (3)	1.3883 (3)
B (cm^{-1})	0.1436683 (3)	0.1435345 (1)	0.1448 (2)
C (cm^{-1})	0.1302251 (3)	0.1302363 (1)	0.1287 (3)
$\Delta_K \times 10^6$ (cm^{-1})	7.2601 (9)	6.11 (10)	[7.2601][c]
$\Delta_{JK} \times 10^7$ (cm^{-1})	−2.311 (5)	−2.53 (2)	−105 (13)
$\Delta_J \times 10^8$ (cm^{-1})	2.708 (8)	2.761 (3)	14 (2)
$\delta_J \times 10^9$ (cm^{-1})	3.08 (7)	2.96 (3)	[3.08][c]
$\delta_K \times 10^7$ (cm^{-1})	1.5 (2)	2.61 (9)	[1.5][c]
ν_0 (cm^{-1})		524.48501 (2)	900.010 (6)
$\Delta\nu_{rms}$ (cm^{-1})	0.00032	0.00029	0.015
κ	−0.97864	−0.97884	−0.9744
No. of lines	2181	1219	185
Max. K'_a	23	6	5
Max. J	67	50	36

[a] Uncertainty (1σ) in the last number is in parentheses.
[b] GSCDs from three bands: 60% from the 524.5-cm^{-1} band; 33% from the 900-cm^{-1} band; 7% from the 907-cm^{-1} band.
[c] GS constants.

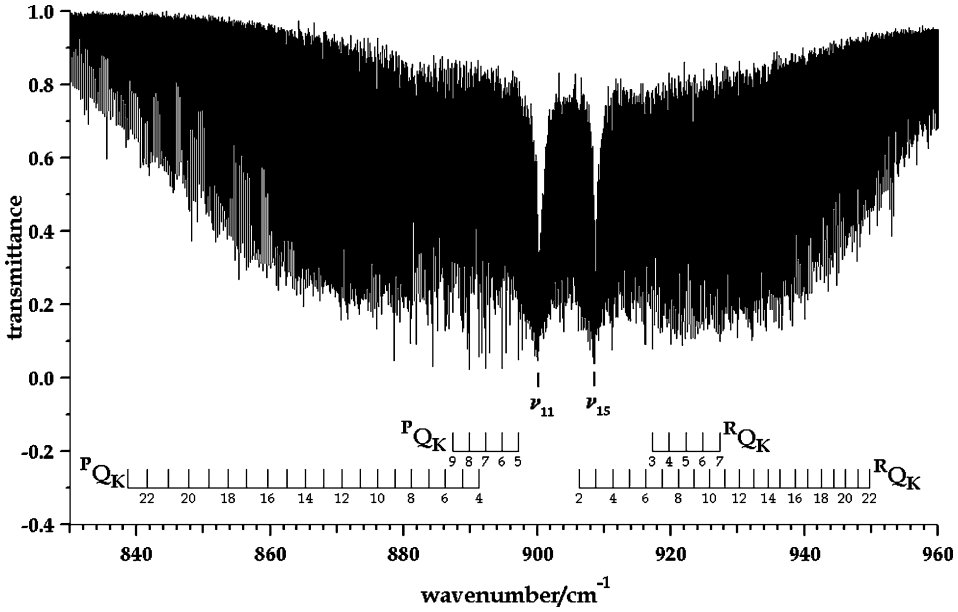

Fig. 5. Overall structure of the overlapping C-type bands of butadiene-1-$^{13}C_1$ near 900 cm^{-1} due to the ν_{11} mode for $^{13}CH_2$ flapping and the ν_{15} mode for $^{12}CH_2$ flapping.

branch in Fig. 6. This figure includes the $^{R}Q_4$, $^{R}Q_5$, and $^{R}Q_6$ features and shows the onset of K_c-splitting in the $^{R}R_3$ series. Assignments in this band include $^{R}R_3$ to $^{R}Q_{22}$ and $^{P}P_4$ to $^{P}P_{23}$ for a total of 1658 lines. From these assignments 712 GSCDs were obtained. These GSCDs for ν_{11} were combined with those for ν_{12} and ν_{15} in the fit of GS rotational constants as given in Table 2. For the ν_{11} band at 900 cm^{-1}, which is strongly perturbed, a rough US fit was done for 185 lines for $^{R}R_K$ and $^{P}P_K$ series with $K'_a \leq 5$. In this fit three of the US constants, Δ_K δ_J, and δ_K were constrained to GS values.

Supplementary Table 1S includes the GSCDs obtained from the C-type band for ν_{11}. Supplementary Table 5S gives lines with $K'_a \leq 5$ and details of fitting the US rotational constants. Supplementary Table 6S gives the remaining 1473 lines with $K'_a > 5$.

A fragmentary assignment was done for the C-type band centered at 909 cm^{-1} due to ν_{15}, the $^{12}CH_2$ flapping mode. Lines were assigned for $^{R}R_3$ to $^{R}R_7$ and $^{P}P_5$ to $^{P}P_9$. These assignments were confined to the lower J values prior to the onset of K_c-splitting. A total of 327 lines were assigned, from which 162 GSCDs were obtained. No fitting of US

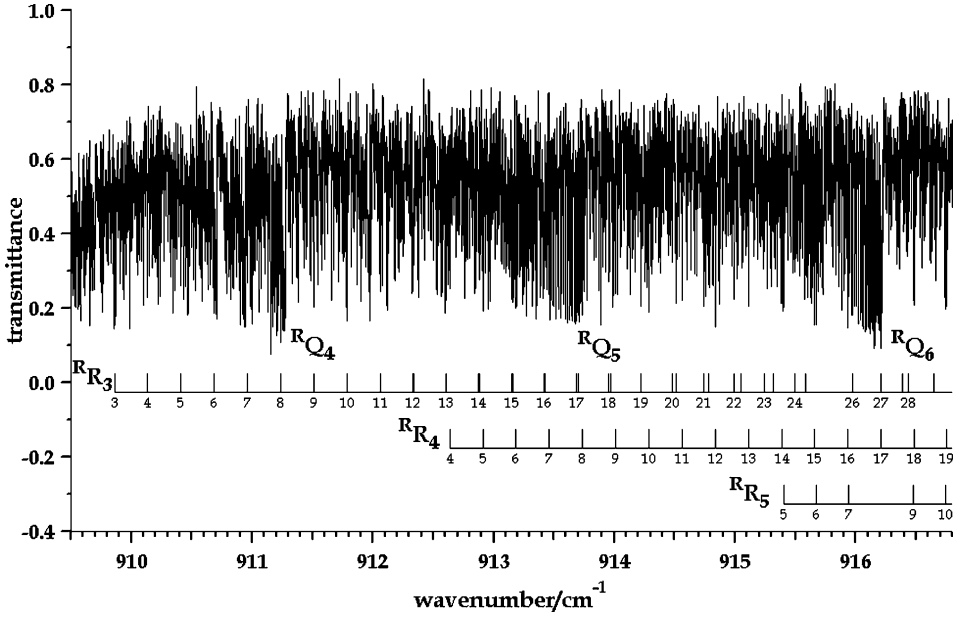

Fig. 6. An example of details of the assignment in the R branch of the band for ν_{11} in the vicinity of $^{R}Q_4$, $^{R}Q_5$, and $^{R}Q_6$.

Table 3
Observed and calculated moments of inertia (a.m.u Å^2) of butadiene, butadiene-2,3-d_2, butadiene-1,1-d_2, and butadiene-1-$^{13}C_1$

	BDE[a]	BDE-2,3-d_2[a]	BDE-1,1-d_2[b]	BDE-1-$^{13}C_1$
Observed				
I_a	12.1244	16.5212	13.8086	12.1383
I_b	113.9805	114.4623	125.0331	117.3372
I_c	126.0910	130.9665	138.8161	129.4499
Δ[c]	−0.0139	−0.0170	−0.0256	−0.0256
Calculated[d]				
I_a	11.91	16.28	13.59	11.92
I_b	114.30	114.79	125.45	117.65
I_c	126.21	131.07	139.04	129.58

[a] Ref. [6].
[b] Ref. [8].
[c] Inertial defect, $\Delta = I_c - I_a - I_b$.
[d] From B3LYP/6-311++G(d,p) calculations. Cartesian coordinates for butadiene in Å: (C_1) $a = -1.80988$, $b = 0.38038$, $c = 0.0$; (C_2) $a = -0.66077$, $b = -0.30575$, $c = 0.0$; (H_1^t) $a = -2.77076$, $b = -0.11990$, $c = 0.0$; (H_1^c) $a = -1.82165$, $b = 1.46593$, $c = 0.0$; (H_2) $a = -0.68944$, $b = -1.39362$, $c = 0.0$. Others by symmetry.

rotational constants was possible for ν_{15}. Supplementary Table 2S includes the GSCDs, which were used in the fit of the GS constants. Supplementary Table 6S contains the assigned lines.

5. Discussion

Ground state rotational constants for butadiene, five deuterium isotopomers, and one ^{13}C isotopomer are now available [6–8]. The corresponding ground state moments of inertia are supplied in Tables 3 and 4. In all cases small inertial defects confirm the planarity of butadiene. Included in the two tables are moments of inertia computed from the equilibrium geometry of butadiene as found with a B3LYP/6-311++G(d,p) model [17]. A footnote in Table 3 gives the Cartesian coordinates of butadiene from the QC calculations. The agreement between the experimental ground state values and the computed equilibrium values is good.

Table 4
Observed and calculated moments of inertia (amu Å^2) of the 1,4-d_2 isotopomers of butadiene

	BDE-t,t-d_2[a]	BDE-c,c-d_2[a]	BDE-c,t-d_2[a]
Observed			
I_a	12.5824	14.7890	13.7654
I_b	128.9808	122.1428	125.4157
I_c	141.5314	136.9090	139.15791
Δ[b]	−0.0319	−0.0229	−0.0232
Calculated[c]			
I_a	12.5777	14.7787	13.7578
I_b	129.6658	122.8886	126.1353
I_c	142.2435	137.6673	139.8931

[a] Ref. [7].
[b] Inertial defect, $\Delta = I_c - I_a - I_b$.
[c] From B3LYP/6-311++G(d,p) calculations.

Experimental data for another ^{13}C species and calculated vibration–rotation constants are needed before an equilibrium structure based on experimental data can be found and compared directly with the structure from the DFT calculation. A preliminary attempt at an r_0 structure fit using the available moments of inertia confirmed that data for ^{13}C substitution at the 2,3 carbons was essential. BDE-2,3-$^{13}C_2$ has been synthesized, and its high-resolution IR spectrum has been recorded. An analysis of the rotational structure in several bands is proceeding. Meanwhile, a normal coordinate analysis of the vibrational fundamentals of all the isotopomers of butadiene is underway with the intention of obtaining vibration–rotation constants for use in extracting equilibrium rotational constants. An equilibrium structure will be fit to these rotational constants, and the effect of pi-electron delocalization on the structure of butadiene will be evaluated.

6. Conclusions

Full investigations of the gas-phase IR spectrum and the liquid-phase Raman spectrum of BDE-1-$^{13}C_1$ have yielded a complete assignment of vibrational fundamentals for this species. The reduced C_s symmetry of BDE-1-$^{13}C_1$ causes two bands corresponding to a_g and b_g modes in the C_{2h} symmetry of butadiene to have significant IR intensity and two bands corresponding to a_u and b_u modes in butadiene to have significant Raman intensity. Ground state rotational constants have been found for BDE-1-$^{13}C_1$ from an analysis of the rotational structure in three C-type bands of the high-resolution IR spectrum. Upper state rotational constants have been fit to lines near the centers of two bands. Once the analysis of the rotational structure in bands of BDE-2,3-$^{13}C_2$ has been completed an equilibrium structure of butadiene should be available with which to test structural consequences of delocalized pi-bonding in butadiene and to evaluate structures predicted by quantum chemical calculations.

Acknowledgements

With this paper we salute Walter J. Lafferty and his wide range of outstanding contributions in high-resolution molecular spectroscopy. RLS was a colleague of Walter Lafferty at the NBS for 28 years, where they worked together on a number of projects in high-resolution molecular spectroscopy. NCC received an excellent start in recording and analyzing high-resolution IR spectra under Walter Lafferty's tutelage. This cooperation began in the summer of 1986 at the NBS. Although Walter Lafferty initially doubted that undergraduates could make useful contributions to such studies, many, including KAH and MCM, have made him a believer during the intervening years.

This research was supported, in part, by the United States Department of Energy, Office of Basic Energy Sciences, Chemical Sciences Division. The high-resolution investigations were performed at the W.R. Wiley Environmental Molecular Science Laboratory, a national scientific user facility sponsored by the Department of Energy's Office of Biological and Environmental Research located at the Pacific Northwest National Laboratory. Pacific Northwest National Laboratory is operated for the United States Department of Energy by Battelle under contract DE-AC06-76RLO 1830.

The work at Oberlin College, including summer stipends for KAH and MCM, was supported by a Camille and Henry Dreyfus Senior Scholar Mentor grant, which we gratefully acknowledge.

We thank Dasan Thamattoor of Colby College for his advice on methods for synthesizing ^{13}C isotopomers of butadiene.

Supplementary Material

Supplementary data associated with this article can be found, in the online version, at doi:10.1016/j.molstruc.2004.11.090

Supplementary Materials include four figures and six tables. The spectra consist Fig. 1aS and bS for the mid-IR region, Fig. 2S for the far-IR region, and Fig. 3S for the Raman spectrum. Table 1S contains details of the assignments in the IR and Raman spectra of butadiene-1-$^{13}C_1$ and the results of the B3LYP/6-311++G(d,p) calculations (3 pages). Table 2S consists of ground state rotational constants fit to GSCDs from 3 C-type bands of butadiene-1-$^{13}C_1$ (12 pages). Table 3S supplies the lines with $K'_a \leq 6$ and their fit to upper state rotational constants fit for the C-type band at 524.5 cm^{-1} of butadiene-1-$^{13}C_1$ (8 pages). Table 4S gives the lines for $K'_a \geq 6$ for the C-type band of butadiene-1-$^{13}C_1$ at 524.5 cm^{-1} (9 pages). Table 5S contains the upper state rotational constants fit to lines with $K'_a \leq 5$ for the C-type band of butadiene-1-$^{13}C_1$ at 900.0 cm^{-1} (2 pages). Table 6S consists of lines for $K'_a \geq 6$ for the C-type band at 900.0 cm^{-1} and all the lines for the C-type band at 909 cm^{-1} for butadiene-1-$^{13}C_1$ (10 pages).

References

[1] P. Groner, in: J.R. Durig (Ed.), Vibrational Spectra and Structure, vol. 24, Elsevier, Amsterdam, 2000 (Chapter 3).
[2] P. Groner, R.D. Warren, J. Mol. Struct. 599 (2001) 323.
[3] A.J. Matzger, K.D. Lewis, C.E. Nathan, A.A. Peebles, R.A. Peebles, R.L. Kuczkowski, J.F. Stanton, J.J. Oh, J. Phys. Chem. A 106 (2002) 12110.
[4] N.C. Craig, P. Groner, D.C. McKean, M.J. Tubergen, Int. J. Quantum Chem. 95 (2003) 837.
[5] J. Demaison, J.E. Boggs, H.D. Rudolph, J. Mol. Struct. 695/696 (2004) 145.
[6] N.C. Craig, J.L. Davis, K.A. Hanson, M.C. Moore, K.J. Weidenbaum, M. Lock, J. Mol. Struct. 695/696 (2004) 59.
[7] N.C. Craig, K.A. Hanson, R.W. Pierce, S.D. Saylor, R.L. Sams, J. Mol. Spectrosc. 228 (2004) 401.
[8] W. Caminati, G. Grassi, A. Bauder, Chem. Phys. Lett. 148 (1988) 13.
[9] M. Halonen, L. Halonen, D.J. Nesbitt, J. Phys. Chem. A 108 (2004) 3367.
[10] Z.-D. Sun, L.-H. Xu, R.M. Lees, X.J. Jiang, S. Perry, N.C. Craig, J. Mol. Struct., (2005) in press.
[11] J.H. Callomon, E. Hirota, T. Iijima, K. Kuchitsu, W.J. Lafferty, in: K.-H. Hellwege, A.M. Hellwege (Eds.), Landolt-Börnstein New Series, Vol. 15 (supplement to volume II17), Springer, Berlin, 1987, p. 412.
[12] P. Huber-Wälchli, Hs.H. Günthard, Spectrochim. Acta 37A (1981) 285.
[13] Yu.N. Panchenko, J. Vander Auwera, Y. Moussaoui, G.R. De Maré, Struct. Chem. 14 (2003) 337.
[14] J.J. Gajewski, K.B. Peterson, J.R. Kagel, Y.C.J. Huang, J. Am. Chem. Soc. 111 (1989) 9078.
[15] A. Maki, T.A. Blake, R.L. Sams, N. Vulpanovici, J. Barber, E.T.H. Chrysostom, A.T. Masiello, J.W. Nibler, A. Weber, J. Mol. Spectrosc. 210 (2001) 240.
[16] Yu. N. Panchenko, first provided normal coordinate and intensity evidence for this conclusion, drawn from his MP2/6-31G* calculations.
[17] M.J. Frisch, G.W. Trucks, H.B. Schlegel, G.E. Scuseria, M.A. Robb, J.R. Cheeseman, V.G. Zakrzewski, J.A. Montgomery, Jr., R.E. Stratmann, J.C. Burant, S. Dapprich, J.M. Millam, A.D. Daniels, K.N. Kudin, M.C. Strain, O. Farkas, J. Tomasi, V. Barone, M. Cossi, R. Cammi, B. Mennucci, C. Pomelli, C. Adamo, S. Clifford, J. Ochterski, G.A. Petersson, P.Y. Ayala, Q. Cui, K. Morokuma, D.K. Malick, A.D. Rabuck, K. Raghavachari, J.B. Foresman, J. Cioslowski, J.V. Ortiz, A.G. Baboul, B.B. Stefanov, G. Liu, A. Liashenko, P. Piskorz, I. Komaromi, R. Gomperts, R.L. Martin, D.J. Fox, T. Keith, M.A. Al-Laham, C.Y. Peng, A. Nanayakkara, M. Challacombe, P.M.W. Gill, B. Johnson, W. Chen, M.W. Wong, J.L. Andres, C. Gonzalez, M. Head-Gordon, E.S. Replogle, J.A. Pople, The DFT calculation was done with the fine grid option, GAUSSIAN 98, Revision A.9 for a PC, Gaussian, Inc., Pittsburgh PA, 1998.
[18] B.P. Winnewisser, J. Reinstädtler, K.M.T. Yamada, J. Behrend, J. Mol. Spectrosc. 136 (1989) 12–16.
[19] C.F. Neese, private communication.